JGR Oceans

RESEARCH ARTICLE
10.1029/2023JC019868

The Kuroshio Intrusion Into the South China Sea at Luzon Strait Can Be Remotely Influenced by the Downstream Intrusion Into the East China Sea

Yuhui Zhao[1,2], X. San Liang[2,3], and Yang Yang[4]

[1]School of Marine Sciences, Nanjing University of Information Science and Technology, Nanjing, China, [2]The Artificial Intelligence Group, Division of Frontier Research, Southern Marine Laboratory, Zhuhai, China, [3]Department of Atmospheric and Oceanic Sciences, Institute of Atmospheric Sciences, Fudan University, Shanghai, China, [4]State Key Laboratory of Marine Environmental Science, College of Ocean and Earth Sciences, Xiamen University, Xiamen, China

Key Points:

- A wake structure southeast of Taiwan usually accompanies the Kuroshio intrusion into the South China Sea
- Influence of the downstream Kuroshio on the wake and further on the upstream Kuroshio intrusion is revealed by a rigorous causality analysis
- Coastal trapped waves are responsible for the counterintuitive downstream-to-upstream causal relation

Correspondence to:
X. S. Liang,
xsliang@fudan.edu.cn

Citation:
Zhao, Y., Liang, X. S., & Yang, Y. (2023). The Kuroshio intrusion into the South China Sea at Luzon Strait can be remotely influenced by the downstream intrusion into the East China Sea. *Journal of Geophysical Research: Oceans*, *128*, e2023JC019868. https://doi.org/10.1029/2023JC019868

Received 24 MAR 2023
Accepted 26 JUL 2023

Abstract The intrusion of Kuroshio into the South China Sea through Luzon Strait has been of enormous interest in western boundary current studies. Here we show that this intrusion can be remotely influenced by the downstream intrusion of the Kuroshio northeast of Taiwan into the East China Sea, at a lead time of about 220 days. This remarkable finding is first revealed by a quantitative causality analysis which is rigorously established from first principles in physics; it is originally motivated by the observation of a wake southeast of Taiwan, whose influence on the loop current, also revealed by causality analysis, is traced downstream to the Kuroshio intrusion into the East China Sea. Further analysis suggests that the two important Kuroshio intrusions are connected via a coastal trapped wave mode with a period of 1.5 years propagating southward along the eastern Taiwan coast, as supported by both theoretical and numerical models. Upon approaching the Luzon Strait, its negative (positive) phase functions to intensify (reduce) the loop current. At a speed of 1.37 km day^{-1}, the mode takes about 220 days for the disturbances northeast of Taiwan to travel along the coast to Luzon Strait, leading to the same time delay for the downstream-upstream causal relation.

Plain Language Summary Kuroshio is the western boundary current of the North Pacific. When the Kuroshio current passes marginal seas including the South China Sea and the East China Sea, branches of the Kuroshio may penetrate into the seas, leading to the well known Kuroshio intrusions. Using a rigorous causality analysis based on information flow, we find that the Kuroshio intrusion into the South China Sea through Luzon Strait can be remotely influenced by the downstream Kuroshio intrusion into the East China Sea. Results show that the influence from the downstream intrusion first reaches a wake structure southeast of Taiwan which usually accompanies the Kuroshio intrusion into the South China Sea, then reaches the upstream intrusion. The causal relation is attributed to one mode of the southward propagating coastal trapped waves along the east coast of Taiwan. Upon approaching the Luzon Strait, its negative (positive) phase functions to intensify (reduce) the loop current, regulating the Kuroshio intrusion on a 1.5-year time scale. Since the speed of the mode is 1.37 km day^{-1}, it takes about 220 days to travel along the coast to Luzon Strait. As a result, the downstream-upstream causal relation has a time delay of about 220 days.

1. Introduction

Kuroshio is one of the most important western boundary currents in the ocean. It originates from the North Equatorial Current and flows northward along the Philippine coast. In passing the Luzon Strait, reportedly Kuroshio may take different paths (e.g., Caruso et al., 2006; Hu et al., 2000; Nan et al., 2011; Yuan et al., 2006), namely, the leaping path, leaking path and looping path (cf. Figure 1). In the first case, the Kuroshio continues to flow northward by leaping across the strait. For the leaking path, a branch of the Kuroshio extends westward into the interior of the South China Sea (SCS); for the looping path, the Kuroshio mainstream forms an anticyclonic loop southwest of Taiwan, and then flows out of the SCS through the northern Luzon Strait. The intrusion of the Kuroshio into the SCS leads to significant exchange of water between the two sides of the strait, as well as complicated eddy-flow interactions, and hence plays a key role in modulating the circulation in the SCS (e.g., Xu & Su, 2000; Xue et al., 2004; Zhao et al., 2016).

The multi-path variability of the Kuroshio at Luzon Strait is a typical feature as revealed when a boundary current passes a lateral gap. It is believed that the strong low-frequency variability is mostly attributed to some internal

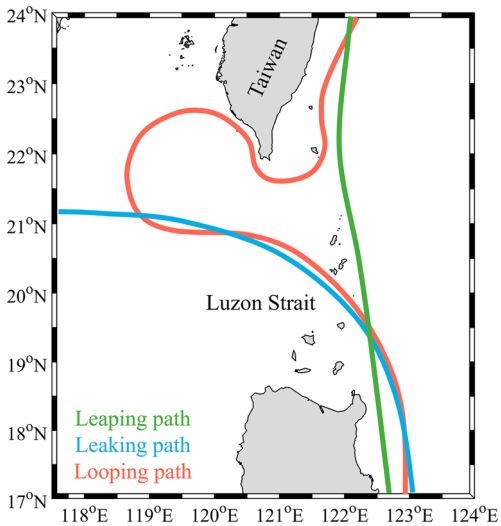

Figure 1. Schematic of the Kuroshio leaping, leaking and looping paths at Luzon Strait.

mechanisms within the boundary current system. Sheremet (2001) applied an idealized model to investigate the flow-gap interaction, and explained the multiple steady states of the boundary current as the competition between beta effect and inertia effect, the former favoring a penetrating state and the latter favoring a leaping state. Moreover, he identified a hysteresis of the nonlinear system: for exactly the same parameters, there may exist different flow states, depending on prior evolutions. A wealth of studies have confirmed the hysteresis and investigated the controlling mechanisms (Gan et al., 2006; Hou et al., 2017; Wu et al., 2016; Yuan, 2002; Yuan et al., 2014). Recently, these paths, that is, the leaping, leaking and looping paths, of a jet through a lateral gap have been observed in laboratory experiments (Pierini et al., 2022). Without change in external forcing and/or boundary condition, these experiments can generate the different paths, providing clear evidence for the self-sustained intrinsic variability of western boundary currents.

While the oscillation of the Kuroshio states could be self-sustained in nature, it is inevitably influenced by external forcings (Cessi, 2021; Chen et al., 2011; Farris & Wimbush, 1996; Kuo et al., 2017; Liang et al., 2019; Metzger & Hurlburt, 2001; Qian et al., 2018). Many studies have reported Kuroshio transitions between the leaping and penetrating paths triggered by local wind as well as mesoscale eddies from the Pacific. Part of the triggering, according to numerical analyses of Wang et al. (2010) and Yuan and Wang (2011), results from the change in meridional advection at a critical state along the hysteresis loop caused by wind or eddies. On the other hand, it is suggested that external forcings could modulate the Kuroshio paths via direct interaction with the current. For example, some studies argue that the wind stress curl southwest of Taiwan offers negative vorticity input whose annual cycle is responsible for the Kuroshio intrusion variability (Sun et al., 2020; Wu & Hsin, 2012; Zhong et al., 2021). And it is believed that cyclonic eddies near the loop current facilitate detachment of anticyclonic eddies from the loop, playing a role in controlling the Kuroshio intrusion (Jia et al., 2005; Zhang et al., 2017; Zhao et al., 2016). This is similar to the Loop Current eddy separation in the Gulf of Mexico (e.g., Nickerson et al., 2022).

In this study, we will present a completely new, and rather counterintuitive, mechanism that may account for part of the intrusion. This is originally motivated by the behavior of a wake southeast of Taiwan, and by a straightforward application of a recently developed causality analysis, which are quantitative in nature and rigorously established from first principles. The rest of the paper is arranged as follows. Section 2 presents the cyclonic wake structure observed from satellite. After that, we define a loop current index in Section 3 for the causal inference that follows. Section 4 begins with a brief introduction of the new quantitative causality analysis, and shows the results of causal inference, by which unexpected downstream factors affecting the Kuroshio intrusion into the SCS are traced. Section 5 investigates the key process responsible for the implementation of the downstream influence. This work is discussed and summarized in Section 6.

2. A Wake Structure of the Kuroshio Loop Current

The looping path, among the three Kuroshio paths, has attracted most attentions in this line of research. Nonetheless, little has been paid to what happens immediately after the Kuroshio loops out of the SCS. One may notice that, as the looping path matures, the northern flank of the Kuroshio loop current (KLC) encounters the southern tip of Taiwan, veering southeastward along the topography (Figure 1). Such encounter of an oceanic current with an obstacle is well known to generate wake eddies in the lee region, over a wide range of scales from O (10^{-1}) to O (10^{1}) of Rossby number (e.g., Chopra & Hubert, 1965; Merrifield et al., 2019; Pattiaratchi et al., 1987; Zheng et al., 2008). However, the wake of the KLC in the lee of the Taiwan Island has been rarely noticed. In the following we will present a satellite-derived map that, for the first time, clearly shows a wake structure of the KLC.

Figure 2a displays the sea surface height (SSH) and geostrophic relative vorticity ζ_g on 4 March 1996, extracted from a widely used altimeter product distributed by Archiving, Validation, and Interpretation of Satellite Oceanographic (AVISO). The data over regions shallower than 100 m are discarded, in case of potential contamination caused by tidal aliasing and other coastal altimetry problems. It is clear from the map that the Kuroshio on this

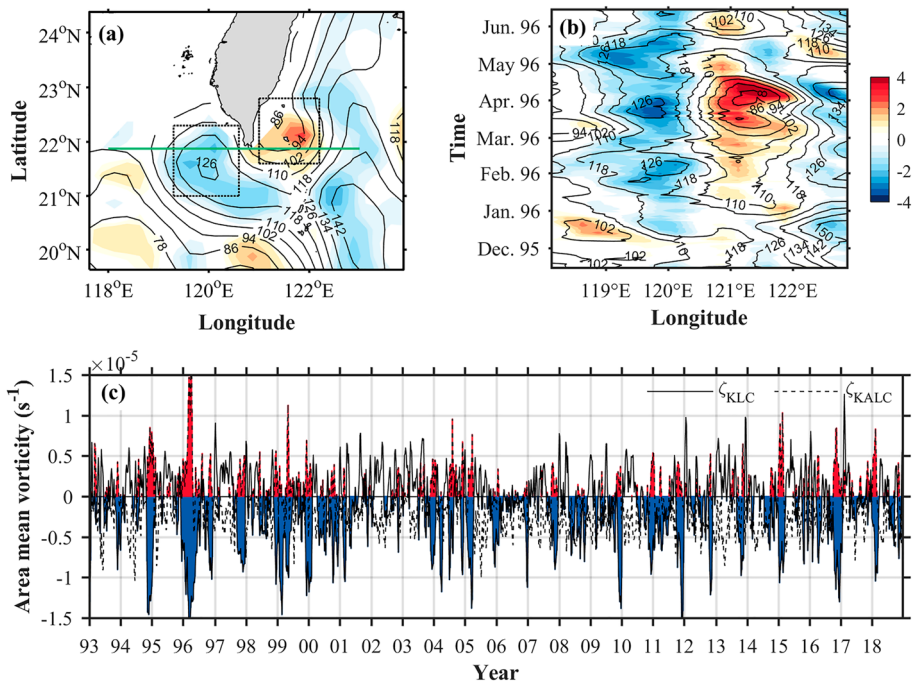

Figure 2. (a) Altimeter-derived map of SSH (contour; cm) and vorticity ζ_g (shading; $\times 10^{-5}$ s^{-1}) on 4 March 1996. (b) Hovmöller diagram of SSH and ζ_g along the green line in (a). Panels (a) and (b) share a common colorbar. (c) The weekly ζ_{KLC} and ζ_{KALC} during 1993–2018 whose negative and positive values are filled with blue and red shadings, respectively. The black dotted boxes in (a) mark regions over which ζ_g is averaged to obtain ζ_{KLC} and ζ_{KALC}.

day takes the looping path. Under the very circumstance, the strong incident KLC is along the southwestern coast of Taiwan, and a large cyclonic wake eddy is induced in the lee, as well identified by the positive ζ_g and closed contours of SSH southeast of Taiwan. In association with the wake eddy is a cyclonic bend of the Kuroshio after leaving the SCS (Figure 2a); it is the same size as the KLC, and, together with it forms a dipole. As indicated by the evolution of SSH and ζ_g along the zonal line passing through the dipole (Figure 2b), the wake structure emerges southeast of Taiwan in January 1996 soon after the KLC develops, then remains stationary, until the KLC starts to decay in early May of the same year. Throughout the whole dipolar event, the cyclonic bending appears as strong as its anticyclonic counterpart. In other words, the newly found wake structure is similar to the KLC, but with an opposite polarity; we hence refer to it as the "Kuroshio anti-loop current" (KALC).

The KALC, a structure in the wake of the KLC, would ideally exist whenever the KLC interacts with the Taiwan Island, which means its occurrence in the first half of 1996 as described above should not be an exception. To further examine the relationship between the loop and anti-loop circulations, ζ_g averaged over the dotted boxes in Figure 2a, designated as ζ_{KLC} and ζ_{KALC}, are used to roughly identify the KLC and KALC, respectively. Negative ζ_{KLC} (positive ζ_{KALC}) loosely corresponds to the occurrence of the KLC (KALC). It shows in Figure 2c that KLCs (blue shadings), regardless of their life durations, are accompanied by KALCs (red shadings) in most cases during 1993–2018. And for each case the companionship persists throughout the whole intrusion duration, as in the afore-mentioned case in 1996 (Figure 2b). The close relationship between KLC and KALC implies a possible interaction in between, and, particularly of our concern, the influence of the latter on the former. To demonstrate whether this is indeed true, we will employ a novel time series causality analysis to fulfill the task. But before doing that, it is necessary to define an appropriate index measuring the KLC behaviors, and that is what will be presented in the following section.

3. Index That Measures the Extent of Kuroshio Intrusion

Several efforts have been devoted to building an index for identifying the variable Kuroshio paths (Huang et al., 2016; Liang et al., 2019; Nan et al., 2011; Wu, 2013; Yu et al., 2013). These proposed indices, though may successfully identify the state of the Kuroshio, are not applicable here for an accurate measurement of the

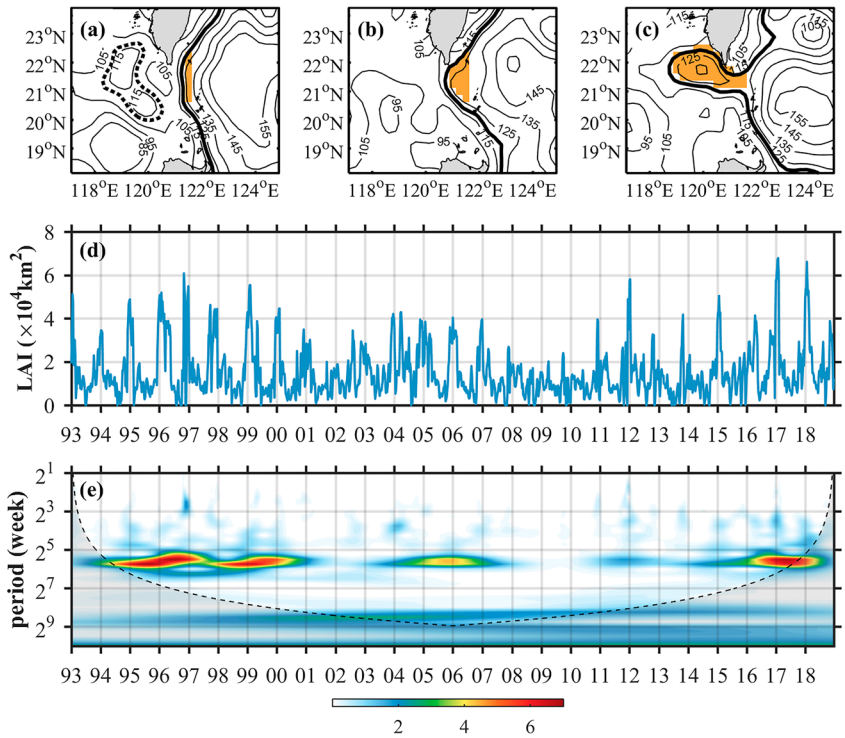

Figure 3. Maps of SSH (cm) on (a) 1 May 2002, (b) 3 November 2002, and (c) 26 October 2016. (d) Weekly LAI during 1993–2018 derived from AVISO. (e) Rectified wavelet power spectrum of the LAI time series. The solid thick contours in (a–c) denote the 120-cm SSH and the shadings cover the looping areas as defined in the text. The dotted thick contour in (a) marks an anticyclonic eddy unrelated to KLC.

very looping path, which is of our concern. Take as an example the widely adopted method by averaging or integrating ζ_g over the KLC region (Huang et al., 2016; Nan et al., 2011; Sun et al., 2020). The index thus obtained may confuse the occasional anticyclonic eddies located in the KLC region (cf. Figure 3a) with the loop current. While a threshold can be set to screen out the misleading values for the mere purpose of path identification, such confusion will cause much error in our causal discovery.

To fix these problems, a new index based on the looping area of KLC is therefore proposed hereafter. We will henceforth refer it to as the looping area index (LAI). It is defined using the isoline of SSH, a good proxy for streamline under the geostrophic assumption. In this study, the 120-cm isoline of SSH is selected to determine the looping area for its proper position within the Kuroshio current. The 120-cm isoline of SSH is, as Figures 3a–3c show, neither so interior as to leak into the SCS sometimes, nor so exterior as to leap across the Luzon strait forever. Notice that there is a cluster of SSH isolines satisfying this criteria. We choose the 120-cm one because the results are more straightforward. The index LAI is then defined as the intersected area (shadings in Figures 3a–3c) of the 120-cm isoline with the 121.5°E meridian along which the island chains are arranged in the Luzon Strait. It should be noticed that the resulting values are referred to as the "looping" area index just in a loose sense, since when the LAI is very small, the 120-cm isoline actually leaps rather than loops, as in the case of Figure 3a.

Figure 3d displays the LAI spanning from 1993 to 2018 derived from AVISO. Its value reflects the intensity of KLC. The greater the value, the deeper the KLC extends into the SCS. When the LAI approaches zero, it means that KLC decays. It is indicated that the index serves as a convincing measure of the KLC variability, at least on seasonal and interannual scales (cf., Figure 3e, the rectified wavelet spectrum, Liu et al., 2007), among others. It peaks generally in winter, reflecting the seasonality of KLC as revealed in previous studies (e.g., Nan et al., 2015; Zhong et al., 2021). Besides, the variation of the KLC intensity from year to year is well presented. Strong KLC events during 1993–2018, as identified by Sun et al. (2020) applying a strict set of criteria, manifest as great peaks of the LAI. Particularly, the documented strongest KLC event in 2016/17 winter since 1993 is clearly shown as a maximum in 2017 January. This event would not stand out as an extreme event if other available indices were used.

4. Causal Discovery Identifies an Unexpected Factor That May Influence the Kuroshio Loop Current

4.1. Quantitative Causality Analysis—Liang-Kleeman Information Flow

To see whether KALC indeed influences KLC, as proposed at the end of Section 2, we employ a rigorously established and, most importantly, quantitative, causality analysis to fulfill the purpose. Causal analysis is an important problem lying at the heart of scientific research. Traditionally it is usually formulated as a statistical testing problem, with only qualitative results offered (e.g., Granger, 1969; Pearl, 2009). During the past 17 years, it has been realized as a physical problem, and can be rigorously established from first principles, rather than axiomatically proposed as ansatz (Liang, 2008, 2013, 2014, 2015, 2016, 2018a, 2019, 2021, 2022; Liang & Kleeman, 2005). That is information flow and the information flow-based causality analysis. As the term "information flow" has been much abused in different disciplines, sometimes it is also referred to as the Liang-Kleeman information flow (L-K information flow henceforth). It merits mentioning that this line of work actually originates from ocean-atmosphere science, and, particularly, atmospheric predictability studies.

The L-K information flow analysis (and hence the entailing causality analysis) has been validated with many benchmark problems in dynamical systems, and has been widely applied with remarkable success in different disciplines, such as the long-term El Niño prediction, CO_2 emission-global warming relation, neural network, quantum entanglement, to name a few (Bai et al., 2018; Hristopulos et al., 2019; Liang et al., 2021; Stips et al., 2016; Yi & Bose, 2022; Zhang & Liang, 2021).

In the rigorous L-K formalism, causality in terms of information flow is regarded as a real physical notion ab initio. Information flow within a given dynamical system, both deterministic and stochastic, first bivariate then generalized to multivariate, has been rigorously derived (Liang, 2016, 2018a), allowing for quantifying the causality between dynamical events. For real-world applications where dynamics is usually unknown and only time series are available, the maximum likelihood estimator of the derived information flow can be obtained. Here for brevity we only show the latter result.

Following Liang (2021), given d time series $X_1, X_2, \ldots, X_d$, the maximum likelihood estimator for the rate of information flow, or simply information flow, from a series X_j to another series X_i (in nats per unit time), is

$$T_{j\to i} = \frac{1}{\det \mathbf{C}} \cdot \sum_{k=1}^{d} \Delta_{jk} C_{k,di} \cdot \frac{C_{ij}}{C_{ii}} \tag{1}$$

where C_{ij} signifies the sample covariance between X_i and X_j, Δ_{jk} stands for the cofactors of the covariance matrix $\mathbf{C} = (C_{ij})$, and $C_{k,di}$ is the sample covariance between X_k and the Euler forward differencing estimation of dX_i/dt. Ideally if $T_{j\to i} \neq 0$, then X_j is causal to X_i; otherwise, if $T_{j\to i} = 0$, then X_j is not causal to X_i (significance test is needed in practice). Its absolute value measures the magnitude of the causality. To obtain the information flow in the opposite direction, one just needs to switch the subscripts i and j in Equation 1.

The formula of the Liang-Kleeman information flow, with only sample covariance involved, is very concise and can be easily computed for efficient causal inference. It has a nice set of properties, including the principle of nil causality (Liang, 2016), the property of asymmetry, the invariance upon coordinate transformation (Liang, 2018a), to name a few. A noteworthy one, among others, is a corollary of Equation 1. When $d = 2$, Equation 1 reduces to

$$T_{2\to 1} = \frac{C_{11}C_{12}C_{2,d1} - C_{12}^2 C_{1,d1}}{C_{11}^2 C_{22} - C_{11}C_{12}^2} = \frac{r}{1-r^2}\left(r_{2,d1}^2 - r r'_{1,d1}\right) \tag{2}$$

where r is the sample correlation coefficient, $r'_{i,dj} = C_{i,dj}/\sqrt{C_{ii}C_{jj}} (i, j = 1, 2)$ is the "correlation" between $\dot{X}_i$ and $\dot{X}_j$ but normalized with the variances of X_i and X_j. It clearly states that causation implies correlation, but not vice versa, fixing with an explicit mathematical expression the long-standing debate over causation versus correlation ever since Berkeley (1710).

4.2. Results of Causality Analysis

Using the L-K information flow-based method, the influence of the local and nonlocal SSH on the KLC behaviors represented by the LAI index is explored. Considering that the Kuroshio east of Taiwan is significantly

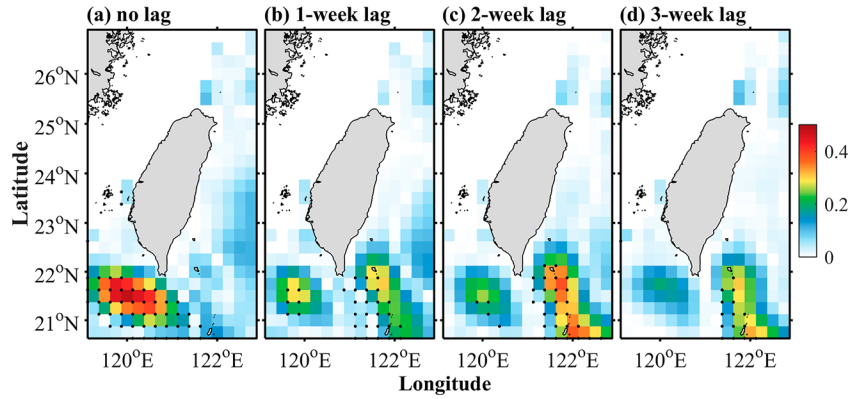

Figure 4. Maps of the normalized absolute information flow from SSH at each grid point to the LAI (a) without lag, and with a lag of (b) 1 week, (c) 2 weeks, and (d) 3 weeks. The scatters mark the information flow significant at a 99% confidence level.

influenced by the westward propagating eddies from the eddy-rich region of the Subtropical Countercurrent (Chang et al., 2015; Chang & Oey, 2011; Qiu, 1999), in which case the eddies may play as a commen driver of the LAI and SSH east of Taiwan and hence result in spurious causality, we here include this factor into our causality analysis. To fulfill this, we follow Chang and Oey (2011) to use the averaged SSH anomaly over the Subtropical Countercurrent region (a tilted parallelogram region east of Taiwan; see Figure 1c therein) to represent the eddy activities (not shown). The time series of the SSH anomaly, together with our focal factors, namely, the LAI index and gridded SSH, constitute a 3-dimensional system at each grid point. The information flow within such a multivariate system then reveals independent causal relations among variables (Liang, 2021). That is to say, the thus-obtained SSH-LAI causality has the influence of the eddies in the Subtropical Countercurrent region excluded. Since the eddies are previously found to be most correlated to the Kuroshio transport with a 6-month delay (Chang & Oey, 2011), the 6-month lagged SSH anomaly is used for causality analysis.

Figure 4a displays the normalized absolute information flow from SSH at each grid point to the LAI index. Thanks to its quantitative nature, the information flow distribution in Figure 4a organizes into a causal structure; here the term "causal structure" follows Liang et al. (2021). The causal structure resembles the KCL-KALC dipole revealed in Figure 2a, having two centers located southwest and southeast of Taiwan, respectively. The former implies that KCL is, beyond doubt, influenced by itself, whereas the latter intriguingly implies that it is also influenced by KALC. While one may notice that the causality from KALC to KLC is weak now, it becomes stronger and significant when a time delay is considered. Shown in Figure 4b is the information flow from SSH to the 1-week lagged LAI. A straightforward observation is the stronger information flow over the east than west centers, indicative of a greater influence on KLC from KALC than from itself. With the time delay increasing, information flow over the east center peaks at a lag time of about 2 weeks (Figure 4c) then rapidly decreases (Figure 4d). The above results suggest that KALC indeed exerts influence on KLC, at a lead time of 2 weeks.

Besides KALC, Figure 4 implies another unexpected source of influence. Albeit weak and insignificant, signals of information flow are found northeast of Taiwan. Following this clue, we further compute the information flow with increasing time delays and eventually identify an information flow center around this region (Figure 5a); its magnitude peaks as the LAI series is lagged by 220 days. More importantly, the corresponding causal structure strikingly resembles the pattern of the Kuroshio intrusion onto the continental shelf of the East China Sea (ECS), which is known as the Kuroshio branch current (KBC; e.g., Qiu & Imasato, 1990; Su et al., 1994; Yang et al., 2012; Cui et al., 2021). Figure 5b indicates that the small loop formed by KBC well coincides with the center of information flow. The coincidence implies that the downstream Kuroshio intrusion into the ECS may influence the upstream Kuroshio intrusion into the SCS, and the influence is generally exerted 220 days in advance.

By now two downstream activities, namely KALC and KBC, are found to be able to influence KLC. By comparing Figures 4c and 5a we notice that KBC, though further downstream located, serves as a larger source of influence on KLC. Furthermore, considering the general traveling times of their influence (2 weeks for KALC and 220 days for KBC) as well as their locations along the Kuroshio current, it naturally occurs to us that KBC may play a more fundamental role in affecting KLC, whereas KALC may just relay in between that mediate. To

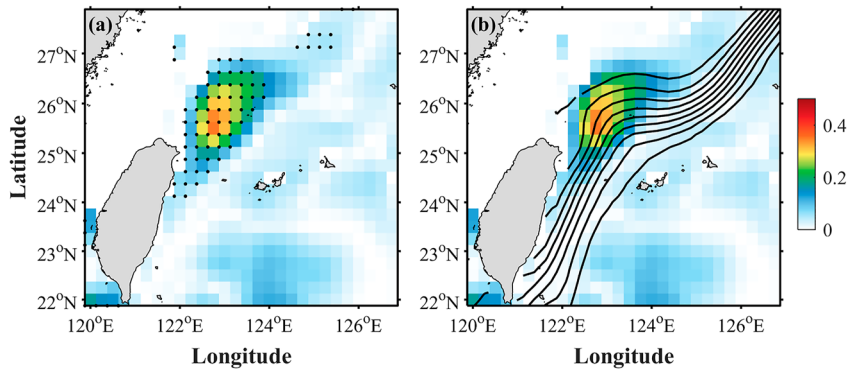

Figure 5. Maps of the normalized absolute information flow from SSH at each grid point to the LAI with a lag of 220 days, where (a) scatters mark the information flow significant at a 99% confidence level and (b) contours denote part of the SSH averaged in winter (JFM).

examine that, time delayed causal relations among the three events are further evaluated. Here KALC and KBC are simply represented by SSH averaged over their respective centers of information flow. The result that KALC and KBC influence KLC at lead times of 15 and 215 days, respectively (Figures 6a and 6b), is consistent with our previous conclusions. Besides, it is noticed that KBC has impact also on KALC (Figure 6c), and the time delay for the maximum influence is 200 days in general. This means that the influence exerted by KBC reaches KALC first after 200 days, and then KLC after 215 days. In this sense, the influence of KALC on KLC could be ultimately traced back to the downstream KBC. Therefore, in the following we will focus on the principal source of influence, namely the downstream Kuroshio intrusion, and investigate the dynamics underlying its causality to the upstream KLC.

5. A New Mechanism Regulating the Kuroshio Loop Current

5.1. Coastal Trapped Waves East of Taiwan

The information flow-based causal inference reveals an unexpected source of influence on KLC, that is, the intrusion of the downstream Kuroshio into the ECS. As Kuroshio flows from south to north, such a countercurrent

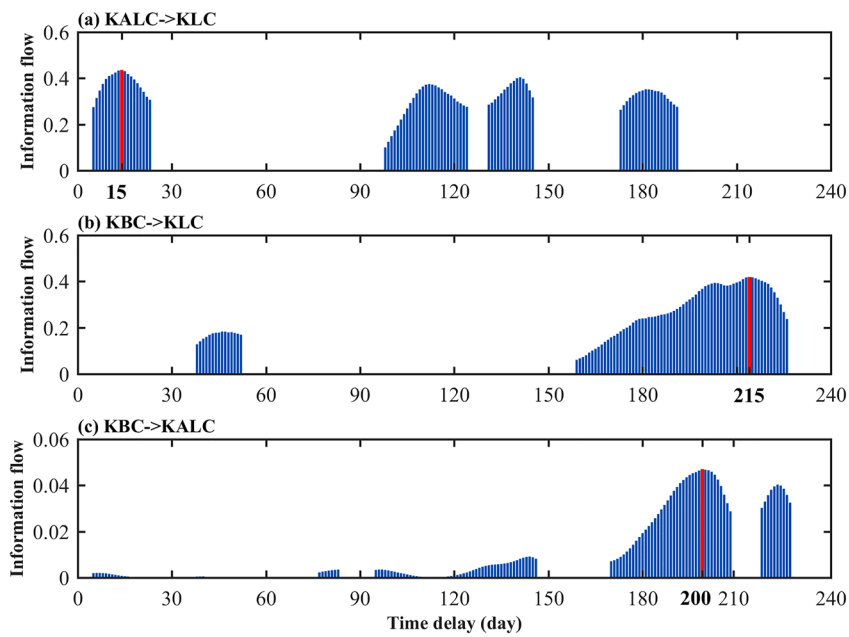

Figure 6. Time delayed information flow significant at a 99% confidence level (a) from KALC to KLC, (b) from KBC to KLC and (c) from KBC to KALC. The red bars denote the maxima.

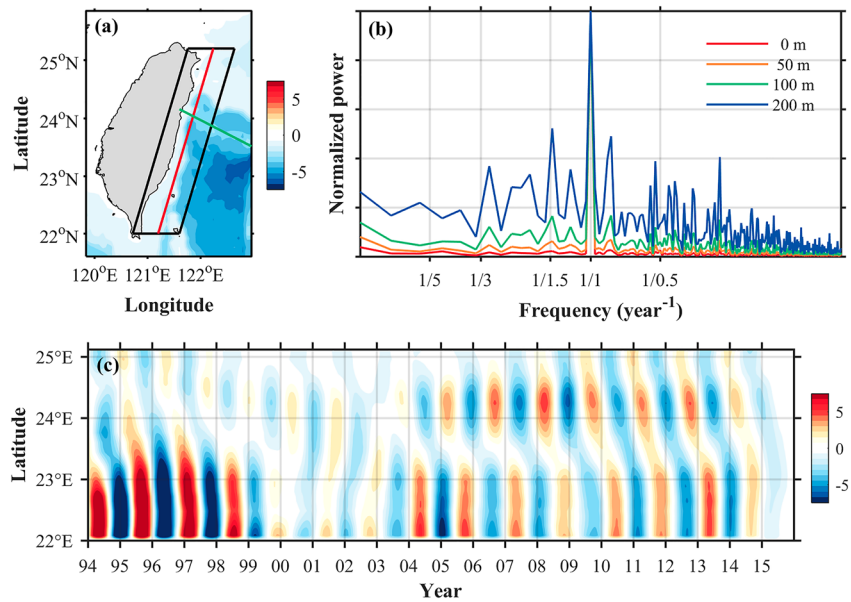

Figure 7. (a) Topography east of Taiwan (km). (b) Normalized power spectrum for velocity averaged over the black solid box in (a) at different depths. (c) Hovmöller diagram of the 490-580-day bandpass filtered meridional velocity (cm s^{-1}) along the red line in (a) at 100 m derived from HYCOM reanalysis. The green line in (a) marks the cross-section S mentioned in the text.

causal path seems unbelievable. However, apart from boundary currents, the coastal ocean can be very complex in dynamics, involving a wealth of processes spanning over the spectrum. The continental slope east of Taiwan, though rather narrow and steep (Figure 7a), allows for rich coastal variabilities as well. As shown in the power spectral analysis for velocity (Figure 7b), processes along the eastern Taiwan coast take place over a broad range of scales, among which the low-frequency part together with the annual signals, makes great contribution. And as the depth increases, the low-frequency variability becomes more dominant. Notice that an output from the Hybrid Coordinate Ocean Model (HYCOM) reanalysis is used from now on, for altimeter product is surface limited and may be contaminated nearshore. Using a hybrid coordinate, HYCOM allows for accurate representations in both deep and shallow regions (Chassignet et al., 2003). The output is 1/12° gridded in horizontal and 40 levels placed in vertical, with a time span from 1994 to 2015, meeting our needs for this purpose.

Among the dominant low-frequency signals stands out the one with 1.5-year period which, as we will see, shows potential ability to realize the countercurrent causal path from downstream. Figure 7c is the Hovmöller diagram of this component along the red line marked in Figure 7a which is roughly parallel to the eastern Taiwan coast; the plotted variable is 490–580 days bandpass filtered meridional velocity. The cutoff periods are such that the component we want is appropriately separated. As the diagram indicates, the 1.5-year component is generally characterized by a southward propagation except in 1998–2003. Leaving aside the abnormal years, the propagating speed of the component is, on average, 1.37 km per day, at which a trip from north to south along the coast (~330 km) takes 240.75 days. This duration is close to the above-obtained 220 days, at an advance of which the downstream intrusion KBC exerts the greatest influence on KLC, as revealed by the causality analysis in Section 4. Therefore, this special low-frequency activity east of Taiwan is likely to be the key to bringing the KBC influence upstream to regulate the KLC behaviors.

The alongshore propagating signal is reminiscent of a well-known wave motion over continental margins, namely, coastal trapped waves (CTWs; Robinson, 1964; Allen, 1975; Wang & Mooers, 1976; Chapman, 1987; Clarke, 1977; Brink, 1991; Zheng et al., 2015; Liang, 2018b). CTWs are a distinctive class of topographically trapped sub-inertial waves, always progressing with the coast on their right in the Northern Hemisphere. They are of paramount importance to remote regulation of coastal processes. Formulated by a set of elegant equations, CTWs can be analytically solved for a class of low-frequency (lower than the inertial frequency) waves when a mean stratification and topography are given, and the long wave assumption is used that the alongshore scale is by far larger than the cross-shelf scale.

Table 1
Celerities (in km per Day) of the Slowest 10 CTW Modes as Solved With a Realistic Topography and Stratification of the Cross-Shore Section S

Mode	M1	M2	M3	M4	M5	M6	M7	M8	M9	M10
C (km day^{-1})	−0.14	−0.29	−0.45	−0.52	−0.58	−0.73	−0.96	−1.31	−1.79	−2.76

Note. The negative sign implies that these waves always propagate southward. The 10 modes from M1 to M10 are in order of increasing magnitude of their respective celerities.

To see whether CTW exists over the eastern shelf of Taiwan, we are here investigating the modal CTW propagation east of Taiwan, which, to our knowledge, has been barely documented. Utilizing the technique by Liang (2018b) (details are seen therein), the free CTWs for the cross-shore section S as marked in Figure 7a are computed. We use the realistic topography of the section, and its stratification is represented by the long-term averaged profile of buoyancy frequency (not shown) derived from HYCOM. Our result of computation shows that CTW with a wide range of propagating speed is possible here. Table 1 lists the celerities of the first 10 slowest trapped modes solved for S. In order of increasing celerities, they are referred to as M1, M2…, respectively. It shows that one CTW mode (M8) propagates southward at a speed of 1.31 km day^{-1}, which is close to the 1.37 km day^{-1} speed associated with the 1.5-year period process as observed and mentioned above.

The above tells that, even with an idealized configuration (e.g., no meridional variation in topography and stratification), the CTW equation does yield an approximately close solution which supports the existence of CTWs east of Taiwan. Hereafter we extract the horizontal and vertical structures of the 1.5-year process out of the HYCOM reanalysis data. Shown in Figure 8 are the horizontal maps of the bimonthly meridional velocity during an episode from December 2012 to October 2014. It indicates that the major signals are coastally trapped and alongshore propagating, which are typical of CTWs. To illustrate, take the negative phase as an example. The coastally trapped signals first appear northeast of Taiwan (Figure 8b) where the Kuroshio crosses the isobath of 100 m to intrude into the ECS and forms KBC, implying the CTWs a result from the Kuroshio intrusion. From the KBC region, the 1.5-year-period CTW mode slowly propagates southwestward along the coast (Figures 8c–8e) and arrives at the southern tip of Taiwan about 8 months later (Figure 8f). Meanwhile, the positive phase of the CTW mode emerges in the KBC region then propagates to the south (Figures 8f–8j). After a period of 1.5 years, new CTWs are excited (Figure 8k), and the above processes repeat. The corresponding evolution over the cross-shore section S implies the same processes (Figure 9). It is noteworthy here that the coastally trapped signals first emerge at the 100-m depth (Figures 9c and 9g) and then extend upward, serving as another evidence for the CTWs to be excited by the interaction of the Kuroshio with the continental shelf (KBC occurs mainly in the subsurface).

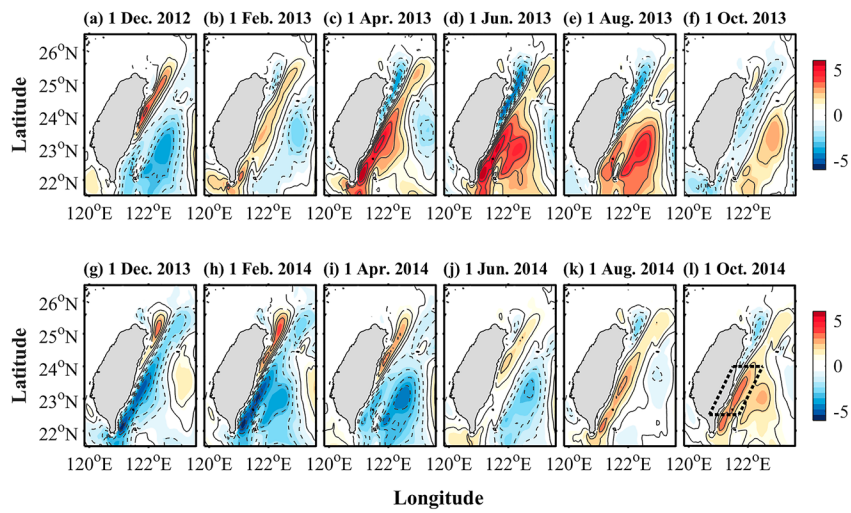

Figure 8. HYCOM-based bimonthly horizontal maps of the 490-580-day bandpass filtered meridional velocity (cm s^{-1}) at 100 m from 1 December 2012 to 1 October 2014.

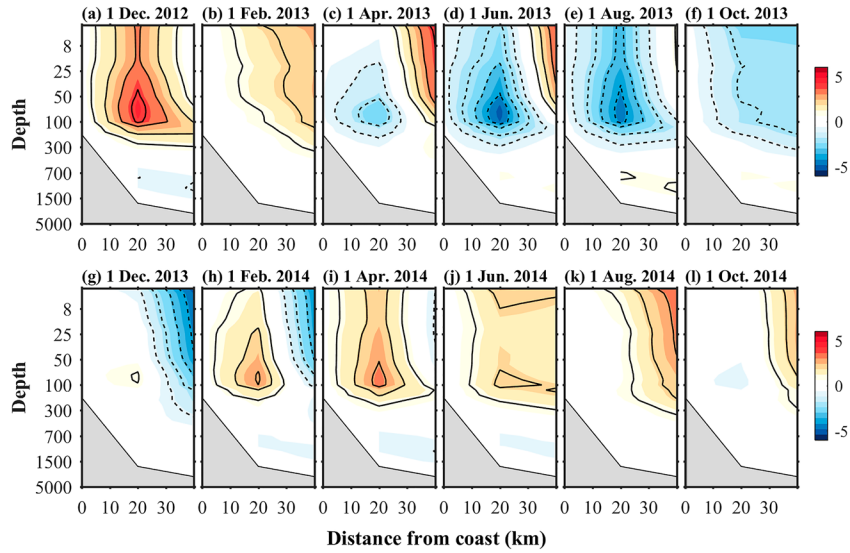

Figure 9. As in Figure 8 but for vertical distributions over the cross-shore section S marked in Figure 7a.

5.2. CTW Effect on the KLC

To illustrate the CTW effect on the KLC, we first compare the LAI index to the meridional velocity averaged along the southeastern Taiwan coast (as marked by the dashed box in Figure 8l). The former measures the KLC events as we introduced in Section 3, and the latter the CTW mode southeast of Taiwan. Both time series are obtained from the HYCOM reanalysis and bandpass filtered with cutoff periods of 490 and 580 days. As shown by Figure 10a, the two series are basically out of phase, indicative of a 1.5-year regulation of the CTW mode over KLC events. Specifically, a negative (positive) phase of the CTW mode southeast of Taiwan corresponds to a strengthened (weakened) KLC event in general.

To further examine the influence of the 1.5-year-period CTW mode on KLC, we perform a composite analysis for different phases of the CTWs. The CTW phases are identified by the threshold of one standard deviation of the velocity time series in Figure 10a: periods with values greater (smaller) than the plus (minus) deviation are selected for the positive (negative) phase composites. This criterion discards the abnormal and weak CTWs. Figures 10b and 10c display velocity and relative vorticity for the two composite phases. It is revealed that as positive CTWs approach, the Kuroshio current shows merely a slight westward bend at the northern Luzon Strait and rapidly returns to its northward path, with a small amount of water intruding into the SCS (Figure 10b). On the contrary, as negative CTWs arrive, the Kuroshio takes the looping path, having a large anticyclonic loop located southwest of Taiwan (Figure 10c). The difference caused by the opposite CTW phases is shown in Figure 10d. It is clear that negative (positive) phase of the CTW mode acts to facilitate (suppress) KLC.

With all the information above, it is now clear how the downstream KBC can influence the upstream KLC 220 days in advance. The cross-shelf intrusion of Kuroshio into the ECS excites certain CTWs northeast of Taiwan, which ideally propagate southward along the eastern coast. Among the CTW modes, the one with a period of 1.5 years plays the dominant role in connecting KBC to KLC. As the particular CTW mode approaches the Luzon Strait, its negative phase functions to intensify KLC, while its positive reduces KLC. This particular mode has a phase speed of 1.37 km day^{-1} on average, and takes approximately 220 days to travel from north to south along the eastern Taiwan coast. As a result, the influence of the downstream KBC on the upstream KLC is generally found to be the largest 220 days later, just as what we discovered early on via the information flow-based causality analysis.

6. Discussion and Conclusions

The Kuroshio loop current (KLC) is a predominant form of Kuroshio intrusion into the South China Sea (SCS). Previously a number of mechanisms have been proposed to explain the formation of this intrusion. In this paper,

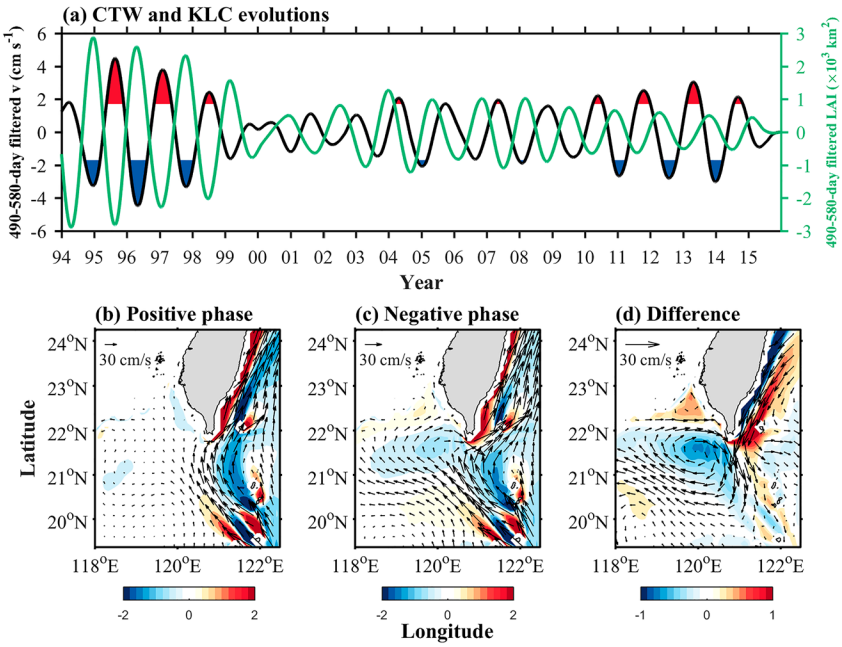

Figure 10. (a) The 490-580-day bandpass filtered LAI and meridional velocity averaged over the dashed box marked in Figure 8l. The 490-580-day bandpass filtered velocity (arrows) and relative vorticity (shadings; $\times 10^{-5}$ s^{-1}) composited for (b) positive and (c) negative phases of the CTW mode. (d) The difference between (b) and (c). The red and blue shadings in (a) denote the periods for the positive and negative phase composites, respectively.

with the aid of a causality analysis, which is quantitative in nature and is rigorously established from first principles in physics, we have inferred an unexpected causal path toward this loop current. The inference is then validated, with dynamical explanation provided.

The work is motivated by the observation of a wake southeast of Taiwan. On encountering with the Taiwan Island, the loop current induces a cyclonic structure in the lee of the island, which is characterized by a mesoscale cyclonic eddy together with a cyclonic bending of the Kuroshio axis southeast of Taiwan. For reference we term the cyclonic structure the "Kuroshio anti-loop current." Application of the Liang-Kleeman information flow-based casual inference reveals that the anti-loop current can influence the loop current about 2 weeks in advance.

Further causal discovery traces the influence of the anti-loop current further downstream to the Kuroshio intrusion northeast of Taiwan into the East China Sea (ECS). It is found, remarkably, that this downstream intrusion impacts on the upstream KLC at a lead time of about 220 days. It is evidenced, from both theoretical investigation and numerical modeling, that this countercurrent causal path along the Taiwan coast is realized by coastal-trapped waves (CTWs) east of Taiwan. It is suggested that the cross-shelf intrusion of the Kuroshio into the ECS excites CTWs northeast of Taiwan; these excited waves then propagate southward along the eastern Taiwan coast. A mode with a period of 1.5 years is observed to be prominent. As the mode approaches Luzon Strait, its negative/positive phase (with southward/northward velocity perturbation) intensifies/reduces the Kuroshio loop current, and hence regulates the Kuroshio intrusion on a 1.5-year time scale. Since this particular CTW mode has a phase speed of 1.37 km per day, it takes a time of approximately 220 days for the perturbation to reach Southeast Taiwan from Northeast Taiwan. As a result, the downstream intrusion into ECS is, unexpectedly, casual to its upstream intrusion into SCS at Luzon Strait, and the causality is approximately, at a lead time of 220 days.

A number of issues remain. By the above observation, the connection between the downstream and upstream Kuroshio intrusions near Taiwan, as well as the influence of the former on the latter, is fulfilled by a certain mode of CTWs east of Taiwan. Then naturally comes a question: Why that mode is selected?

One possible explanation of the selection of the 1.5-year-period CTW mode is its synchronization with the eddies of the same period in the KLC region, which seemingly belong to a pattern known as the Rossby normal modes (RNMs; e.g., Pedlosky & Spall, 1999; Graef, 2016; Xie et al., 2018). Shown in Figure 11 are two snapshots of

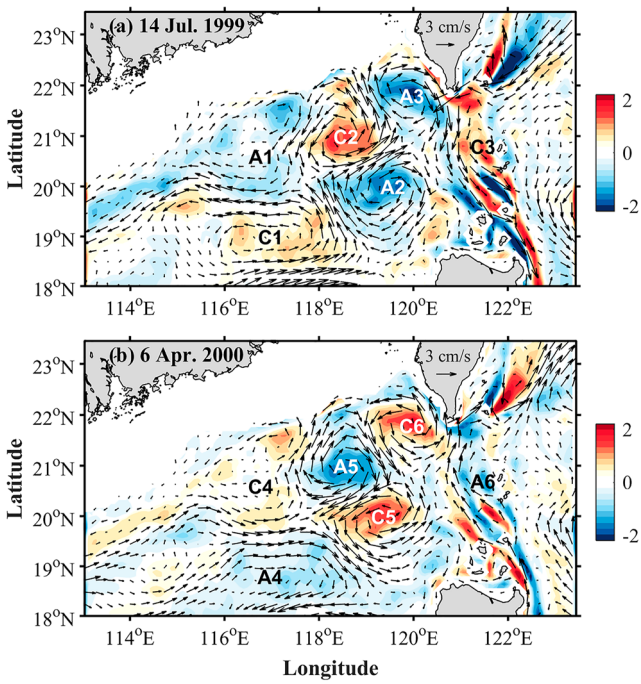

Figure 11. The 490-580-day bandpass filtered velocity (arrows) and relative vorticity (shadings; $\times 10^{-5}$ s^{-1}) at 100 m on (a) 14 July 1999 and (b) 6 April 2000 (from HYCOM).

the bandpass filtered velocity and corresponding relative vorticity on 14 July 1999 and 6 April 2000, respectively. The cutoff periods remain the same as 490 and 580 days. The most conspicuous feature of the maps is a regular distribution of eddies west of the Luzon Strait. These eddies are basically of the same size and alternatively arranged in a chessboard pattern resembling RNMs which, though not documented before in the northeastern SCS, are suggested to be favored by resonance of the SCS waterbody with the incoming long waves from the Pacific (cf. Xie et al., 2018). The RNM-like pattern propagates southwestward along the topography, so cyclonic and anticyclonic eddies alternatively occupy the same area (Figure 11).

With the same period, the RNM, especially its component southwest of Taiwan, and the CTW mode somehow seem to be synchronized. A positive (negative) CTW southeast of Taiwan well corresponds to a cyclonic (an anticyclonic) eddy southwest of Taiwan; they jointly cause northward (southward) velocity which weakens (strengthens) the Kuroshio current, and thus facilitates (suppresses) KLC, in agreement with previous studies (Gan et al., 2006; Wu et al., 2016; Yuan et al., 2014). The cooperation between the RNM and CTW mode could be interpreted as a process of selection. The CTW mode, for its synchronization with the 1.5-year-period RNM, stands out to exhibit the greatest influence on KLC, and eventually determine the time delay of 220 days, while other modes, as they lack cooperation from the RNM, would make less significant contributions, if any.

Data Availability Statement

The merged product of satellite altimeters distributed by Archiving, Validation, and Interpretation of Satellite Oceanographic (CMEMS, 2019) and the output from the Hybrid Coordinate Ocean Model reanalysis (HYCOM, 2021) were used in the creation of this manuscript. The AVISO data was available at https://marine.copernicus.eu. The HYCOM reanalysis data was publicly available at https://www.hycom.org. Figures were made with Matlab version R2021b (Mathworks, 2021).

Acknowledgments

This work was supported by the National Natural Science Foundation of China (Grants. 42230105, 41975064, and 42276017), by Southern Marine Science and Engineering Guangdong Laboratory (Zhuhai) through the Startup Foundation (Grant 313022005), by Shanghai B & R Joint Laboratory Project (Grant 22230750300), and by Shanghai International Science and Technology Partnership Project (Grant 21230780200).

References

Allen, J. S. (1975). Coastal trapped waves in a stratified ocean. *Journal of Physical Oceanography*, *5*(2), 300–325. https://doi.org/10.1175/1520-0485(1975)005<0300:CTWIAS>2.0.CO;2

Bai, C., Zhang, R., Bao, S., San Liang, X., & Guo, W. (2018). Forecasting the tropical cyclone genesis over the northwest Pacific through identifying the causal factors in cyclone–climate interactions. *Journal of Atmospheric and Oceanic Technology*, *35*(2), 247–259. https://doi.org/10.1175/JTECH-D-17-0109.1

Berkeley, G. (1710). A treatise concerning the principles of human knowledge.

Brink, K. H. (1991). Coastal-trapped waves and wind-driven currents over the continental shelf. *Annual Review of Fluid Mechanics*, *23*(1), 389–412. https://doi.org/10.1146/annurev.fl.23.010191.002133

Caruso, M. J., Gawarkiewicz, G. G., & Beardsley, R. C. (2006). Interannual variability of the Kuroshio intrusion in the South China Sea. *Journal of Oceanography*, *62*(4), 559–575. https://doi.org/10.1007/s10872-006-0076-0

Cessi, P. (2021). Gulf Stream and Kuroshio synchronization. *Science*, *374*(6565), 259–260. https://doi.org/10.1126/science.abl9133

Chang, Y.-L., Miyazawa, Y., & Guo, X. (2015). Effects of the STCC eddies on the Kuroshio based on the 20-year JCOPE2 reanalysis results. *Progress in Oceanography*, *135*, 64–76. https://doi.org/10.1016/j.pocean.2015.04.006

Chang, Y.-L., & Oey, L.-Y. (2011). Interannual and seasonal variations of Kuroshio transport east of Taiwan inferred from 29 years of tide-gauge data. *Geophysical Research Letters*, *38*(8), L08603. https://doi.org/10.1029/2011GL047062

Chapman, D. C. (1987). Application of wind-forced, long, coastal-trapped wave theory along the California coast. *Journal of Geophysical Research*, *92*(C2), 1798–1816. https://doi.org/10.1029/JC092iC02p01798

Chassignet, E. P., Smith, L. T., Halliwell, G. R., & Bleck, R. (2003). North Atlantic simulations with the hybrid coordinate ocean model (HYCOM): Impact of the vertical coordinate choice, reference pressure, and thermobaricity. *Journal of Physical Oceanography*, *33*(12), 2504–2526. https://doi.org/10.1175/1520-0485(2003)033<2504:NASWTH>2.0.CO;2

Chen, G., Hu, P., Hou, Y., & Chu, X. (2011). Intrusion of the Kuroshio into the South China Sea, in September 2008. *Journal of Oceanography*, *67*(4), 439–448. https://doi.org/10.1007/s10872-011-0047-y

Chopra, K. P., & Hubert, L. F. (1965). Mesoscale eddies in wake of islands. *Journal of the Atmospheric Sciences*, *22*(6), 652–657. https://doi.org/10.1175/1520-0469(1965)022<0652:MEIWOI>2.0.CO;2

Clarke, A. J. (1977). Observational and numerical evidence for wind-forced coastal trapped long waves. *Journal of Physical Oceanography*, *7*(2), 231–247. https://doi.org/10.1175/1520-0485(1977)0072.0.CO;2

CMEMS. (2019). Global ocean gridded L4 sea surface heights and derived variables reprocessed 1993 ongoing [Dataset]. Copernicus Marine and Environment Monitoring Service (CMEMS). https://doi.org/10.48670/moi-00148

Cui, X., Yang, D., Sun, C., Feng, X., Gao, G., Xu, L., & Yin, B. (2021). New insight into the onshore intrusion of the Kuroshio into the East China Sea. *Journal of Geophysical Research: Oceans*, *126*(2), e2020JC016248. https://doi.org/10.1029/2020JC016248

Farris, A., & Wimbush, M. (1996). Wind-induced Kuroshio intrusion into the South China Sea. *Journal of Oceanography*, *52*(6), 771–784. https://doi.org/10.1007/BF02239465

Gan, J., Li, H., Curchitser, E. N., & Haidvogel, D. B. (2006). Modeling South China Sea circulation: Response to seasonal forcing regimes. *Journal of Geophysical Research*, *111*(C6), C06034. https://doi.org/10.1029/2005JC003298

Graef, F. (2016). Free and forced Rossby normal modes in a rectangular gulf of arbitrary orientation. *Dynamics of Atmospheres and Oceans*, *75*, 46–57. https://doi.org/10.1016/j.dynatmoce.2016.05.005

Granger, C. W. J. (1969). Investigating causal relations by econometric models and crossspectral methods. *Econometrica*, *37*(3), 424–438. https://doi.org/10.2307/1912791

Hou, Y. J., Liu, Y. H., Po, H. U., & Wang, Z. (2017). Nonlinear dynamics of Kuroshio intrusion in the Luzon Strait. *Science China Earth Sciences*, *060*(004), 761–769. https://doi.org/10.1007/s11430-016-9012-7

Hristopulos, D. T., Babul, A., Babul, S., Brucar, L. R., & Virji-Babul, N. (2019). Disrupted information flow in resting-state in adolescents with sports related concussion. *Frontiers in Human Neuroscience*, *13*, 419. https://doi.org/10.3389/fnhum.2019.00419

Hu, J., Kawamura, H., Hong, H., & Qi, Y. (2000). A review on the currents in the South China Sea: Seasonal circulation, South China Sea warm current and Kuroshio intrusion. *Journal of Oceanography*, *56*(6), 607–624. https://doi.org/10.1023/a:1011117531252

Huang, Z., Liu, H., Hu, J., & Lin, P. (2016). A double-index method to classify Kuroshio intrusion paths in the Luzon Strait. *Advances in Atmospheric Sciences*, *33*(6), 715–729. https://doi.org/10.1007/s00376-015-5171-y

HYCOM. (2021). Global ocean forecasting system (version 3.1) [Dataset]. Naval Research Laboratory. Retrieved from https://www.hycom.org/dataserver/gofs-3pt1/reanalysis

Jia, Y., Liu, Q., & Liu, W. (2005). Primary study of the mechanism of eddy shedding from the Kuroshio bend in Luzon Strait. *Journal of Oceanography*, *61*(6), 1017–1027. https://doi.org/10.1007/s10872-006-0018-x

Kuo, Y. C., Chern, C. S., & Zheng, Z. W. (2017). Numerical study on the interactions between the Kuroshio current in the Luzon Strait and a mesoscale eddy. *Ocean Dynamics*, *67*(3–4), 369–381. https://doi.org/10.1007/s10236-017-1038-3

Liang, P., Mu, M., Wang, Q., & Yang, L. (2019). Optimal precursors triggering the Kuroshio Intrusion into the South China Sea obtained by the conditional nonlinear optimal perturbation approach. *Journal of Geophysical Research: Oceans*, *124*(6), 3941–3962. https://doi.org/10.1029/2018JC014545

Liang, X. S. (2008). Information flow within stochastic dynamical systems. *Physical Review E*, *78*(3), 031113. https://doi.org/10.1103/PhysRevE.78.031113

Liang, X. S. (2013). The Liang-Kleeman information flow: Theory and applications. *Entropy*, *15*(1), 327–360. https://doi.org/10.3390/e15010327

Liang, X. S. (2014). Unraveling the cause-effect relation between time series. *Physical Review E*, *90*(5), 052150. https://doi.org/10.1103/PhysRevE.90.052150

Liang, X. S. (2015). Normalizing the causality between time series. *Physical Review*, *6*(2), 022126. https://doi.org/10.1103/physreve.92.022126

Liang, X. S. (2016). Information flow and causality as rigorous notions *ab initio*. *Physical Review E*, *94*(5), 052201. https://doi.org/10.1103/PhysRevE.94.052201

Liang, X. S. (2018a). Causation and information flow with respect to relative entropy. *Chaos: An Interdisciplinary Journal of Nonlinear Science*, *28*(7), 075311. https://doi.org/10.1063/1.5010253

Liang, X. S. (2018b). The slow coastal-trapped waves off Subei Bank in the Yellow Sea and their climatic change in the past decades. In X. S. Liang & Y. Zhang (Eds.), *Coastal environment, disaster, and infrastructure - A case study of China's coastline*. InTech. https://doi.org/10.5772/intechopen.80017

Liang, X. S. (2019). A study of the cross-scale causation and information flow in a stormy model mid-latitude atmosphere. *Entropy*, *21*(2), 149. https://doi.org/10.3390/e21020149

Liang, X. S. (2021). Normalized multivariate time series causality analysis and causal graph reconstruction. *Entropy*, *23*(6), 679. https://doi.org/10.3390/e23060679

Liang, X. S. (2022). The causal interaction between complex subsystems. *Entropy*, *24*(1), 3. https://doi.org/10.3390/e24010003

Liang, X. S., & Kleeman, R. (2005). Information transfer between dynamical system components. *Physical Review Letters*, *95*(24), 244101. https://doi.org/10.1103/PhysRevLett.95.244101

Liang, X. S., Xu, F., Rong, Y., Zhang, R., Tang, X., & Zhang, F. (2021). El Niño Modoki can be mostly predicted more than 10 years ahead of time. *Scientific Reports*, *11*(1), 17860. https://doi.org/10.1038/s41598-021-97111-y

Liu, Y., Liang, X. S., & Weisberg, R. H. (2007). Rectification of the bias in the wavelet power spectrum. *Journal of Atmospheric and Oceanic Technology*, *24*(12), 2093–2102. https://doi.org/10.1175/2007JTECHO511.1

Mathworks (2021). Matlab R2021b [Software]. Mathworks. https://ww2.mathworks.cn

Merrifield, S., Colin, P., Cook, T., Garcia-Moreno, C., MacKinnon, J., Otero, M., et al. (2019). Island wakes observed from high-frequency current mapping radar. *Oceanography*, *32*(4), 92–101. https://doi.org/10.5670/oceanog.2019.415

Metzger, E. J., & Hurlburt, H. E. (2001). The nondeterministic nature of Kuroshio penetration and eddy shedding in the South China Sea. *Journal of Physical Oceanography*, *31*(7), 1712–1732. https://doi.org/10.1175/1520-0485(2001)031<1712:tnnokp>2.0.co;2

Nan, F., Xue, H., Chai, F., Shi, L., Shi, M., & Guo, P. (2011). Identification of different types of Kuroshio intrusion into the South China Sea. *Ocean Dynamics*, *61*(9), 1291–1304. https://doi.org/10.1007/s10236-011-0426-3

Nan, F., Xue, H., & Yu, F. (2015). Kuroshio intrusion into the South China Sea: A review. *Progress in Oceanography*, *137*, 314–333. (SEP.PT.A). https://doi.org/10.1016/j.pocean.2014.05.012

Nickerson, A., Weisberg, R., & Liu, Y. (2022). On the evolution of the Gulf of Mexico loop current through its penetrative, ring shedding and retracted states. *Advances in Space Research*, *69*(11), 4058–4077. https://doi.org/10.1016/j.asr.2022.03.039

Pattiaratchi, C., James, A., & Collins, M. (1987). Island wakes and headland eddies: A comparison between remotely sensed data and laboratory experiments. *Journal of Geophysical Research*, *92*(C1), 783–794. https://doi.org/10.1029/JC092iC01p00783

Pearl, J. (2009). *Causality: Models, reasoning, and inference* (2nd ed.). Cambridge University Press.

Pedlosky, J., & Spall, M. (1999). Rossby normal modes in basins with barriers. *Journal of Physical Oceanography*, *29*(9), 2332–2349. https://doi.org/10.1175/1520-0485(1999)029<2332:RNMIBW>2.0.CO;2

Pierini, S., de Ruggiero, P., Negretti, M. E., Schiller-Weiss, I., Weiffenbach, J., Viboud, S., et al. (2022). Laboratory experiments reveal intrinsic self-sustained oscillations in ocean relevant rotating fluid flows. *Scientific Reports*, *12*(1), 1375. https://doi.org/10.1038/s41598-022-05094-1

Qian, S., Wei, H., Xiao, J., & Nie, H. (2018). Impacts of the Kuroshio intrusion on the two eddies in the northern South China Sea in late spring 2016. *Ocean Dynamics*, *68*(12), 1695–1709. https://doi.org/10.1007/s10236-018-1224-y

Qiu, B. (1999). Seasonal eddy field modulation of the North Pacific subtropical countercurrent: TOPEX/POSEIDON observations and theory. *Journal of Physical Oceanography*, *29*(10), 2471–2486. https://doi.org/10.1175/1520-0485(1999)029<2471:sefmot>2.0.co;2

Qiu, B., & Imasato, N. (1990). A numerical study on the formation of the Kuroshio counter current and the Kuroshio Branch current in the East China Sea. *Continental Shelf Research*, *10*(2), 165–184. https://doi.org/10.1016/0278-4343(90)90028-K

Robinson, A. R. (1964). Continental shelf waves and the response of sea level to weather systems. *Journal of Geophysical Research*, *69*(2), 367–368. https://doi.org/10.1029/JZ069i002p00367

Sheremet, V. A. (2001). Hysteresis of a western boundary current leaping across a gap. *Journal of Physical Oceanography*, *31*(5), 1247–1259. https://doi.org/10.1175/1520-0485(2001)031<1247:HOAWBC>2.0.CO;2

Stips, A., Macias, D., Coughlan, C., Garcia-Gorriz, E., & Liang, X. S. (2016). On the causal structure between CO2 and global temperature. *Scientific Reports*, *6*(1), 21691. https://doi.org/10.1038/srep21691

Su, J., Pan, Y., & Liang, X. S. (1994). Kuroshio intrusion and Taiwan warm current. *Oceanology of China Seas*, *1*, 59–70.

Sun, Z., Zhang, Z., Qiu, B., Zhang, X., Zhou, C., Huang, X., et al. (2020). Three-dimensional structure and interannual variability of the Kuroshio loop current in the Northeastern South China Sea. *Journal of Physical Oceanography*, *50*(9), 2437–2455. https://doi.org/10.1175/JPO-D-20-0058.1

Wang, D.-P., & Mooers, C. N. K. (1976). Coastal-trapped waves in a continuously stratified ocean. *Journal of Physical Oceanography*, *6*(6), 853–863. https://doi.org/10.1175/1520-0485(1976)006<0853:CTWIAC>2.0.CO;2

Wang, Z., Yuan, D., & Hou, Y. (2010). Effect of meridional wind on gap-leaping western boundary current. *Chinese Journal of Oceanology and Limnology*, *28*(2), 354–358. https://doi.org/10.1007/s00343-010-9281-1

Wu, C.-R. (2013). Interannual modulation of the Pacific Decadal Oscillation (PDO) on the low-latitude western North Pacific. *Progress in Oceanography*, *110*, 49–58. https://doi.org/10.1016/j.pocean.2012.12.001

Wu, C.-R., & Hsin, Y.-C. (2012). The forcing mechanism leading to the Kuroshio intrusion into the South China Sea. *Journal of Geophysical Research*, *117*(C7), C07015. https://doi.org/10.1029/2012JC007968

Wu, C.-R., Wang, Y.-L., Lin, Y.-F., Chiang, T.-L., & Wu, C.-C. (2016). Weakening of the Kuroshio intrusion into the South China Sea under the global warming hiatus. *IEEE Journal of Selected Topics in Applied Earth Observations and Remote Sensing*, *9*(11), 5064–5070. https://doi.org/10.1109/JSTARS.2016.2574941

Xie, L., Zheng, Q., Zhang, S., Hu, J., Li, M., Li, J., & Xu, Y. (2018). The Rossby normal modes in the South China Sea deep basin evidenced by satellite altimetry. *International Journal of Remote Sensing*, *39*(1–2), 399–417. https://doi.org/10.1080/01431161.2017.1384591

Xu, J., & Su, J. (2000). Hydrological analysis of Kuroshio water intrusion into the South China Sea. *Acta Oceanologica Sinica*, *19*, 1–21.

Xue, H., Chai, F., Pettigrew, N., Xu, D., Shi, M., & Xu, J. (2004). Kuroshio intrusion and the circulation in the South China Sea. *Journal of Geophysical Research*, *109*(C2), C02017. https://doi.org/10.1029/2002JC001724

Yang, D., Yin, B., Liu, Z., Bai, T., Qi, J., & Chen, H. (2012). Numerical study on the pattern and origins of Kuroshio branches in the bottom water of southern East China Sea in summer. *Journal of Geophysical Research*, *117*(C2), C02014. https://doi.org/10.1029/2011JC007528

Yi, B., & Bose, S. (2022). Quantum Liang information flow as causation quantifier. *Physical Review Letters*, *129*(2), 020501. https://doi.org/10.1103/PhysRevLett.129.020501

Yu, X., Wang, F., & Wan, X. (2013). Index of Kuroshio penetrating the Luzon Strait and its preliminary application. *Acta Oceanologica Sinica*, *32*(1), 1–11. https://doi.org/10.1007/s13131-013-0262-z

Yuan, D. (2002). A numerical study of the South China Sea deep circulation and its relation to the Luzon Strait transport. *Acta Oceanologica Sinica*, *21*, 187–202.

Yuan, D., Han, W., & Hu, D. (2006). Surface Kuroshio path in the Luzon Strait area derived from satellite remote sensing data. *Journal of Geophysical Research*, *111*(C11), C11007. https://doi.org/10.1029/2005JC003412

Yuan, D., & Wang, Z. (2011). Hysteresis and dynamics of a western boundary current flowing by a gap forced by impingement of mesoscale eddies. *Journal of Physical Oceanography*, *41*(5), 878–888. https://doi.org/10.1175/2010JPO4489.1

Yuan, Y., Tseng, Y.-H., Yang, C., Liao, G., Chow, C. H., Liu, Z., et al. (2014). Variation in the Kuroshio intrusion: Modeling and interpretation of observations collected around the Luzon Strait from July 2009 to March 2011. *Journal of Geophysical Research: Oceans*, *119*(6), 3447–3463. https://doi.org/10.1002/2013JC009776

Zhang, Y., & Liang, X. S. (2021). The causal role of South China Sea on the Pacific–North American teleconnection pattern. *Climate Dynamics*, *59*(5–6), 1815–1832. https://doi.org/10.1007/s00382-021-06070-7

Zhang, Z., Zhao, W., Qiu, B., & Tian, J. (2017). Anticyclonic eddy sheddings from Kuroshio loop and the accompanying cyclonic eddy in the northeastern South China Sea. *Journal of Physical Oceanography*, *47*(6), 1243–1259. https://doi.org/10.1175/JPO-D-16-0185.1

Zhao, Y.-B., Liang, X. S., & Gan, J. (2016). Nonlinear multiscale interactions and internal dynamics underlying a typical eddy-shedding event at Luzon Strait. *Journal of Geophysical Research: Oceans*, *121*(11), 8208–8229. https://doi.org/10.1002/2016JC012483

Zheng, Q., Lin, H., Meng, J., Hu, X., Song, Y. T., Zhang, Y., & Li, C. (2008). Sub-mesoscale ocean vortex trains in the Luzon Strait. *Journal of Geophysical Research*, *113*(C4), C04032. https://doi.org/10.1029/2007JC004362

Zheng, Q., Zhu, B., Li, J., Sun, Z., Xu, Y., & Hu, J. (2015). Growth and dissipation of typhoon-forced solitary continental shelf waves in the northern South China Sea. *Climate Dynamics*, *45*(3–4), 1–13. https://doi.org/10.1007/s00382-014-2318-y

Zhong, Y., Zhou, M., Waniek, J. J., Zhou, L., & Zhang, Z. (2021). Seasonal variation of the surface Kuroshio intrusion into the South China Sea evidenced by satellite geostrophic streamlines. *Journal of Physical Oceanography*, *51*(8), 2705–2718. https://doi.org/10.1175/JPO-D-20-0242.1